Article

Discovery Medicine 2024; 36(189): 2046–2054
https://doi.org/10.24976/Discov.Med.202436189.188

SIRT2 Alleviates Inflammatory Response, Apoptosis, and ECM Degradation in Osteoarthritic Chondrocytes by Stabilizing *PCK1*

Fan Zhong[1], Shiqiang Cen[1], Cheng Long[1], Lin Teng[2], Gang Zhong[1,*]

[1]Department of Orthopedic Surgery, West China Hospital, Sichuan University/Trauma Center, West China Hospital, Sichuan University, 610041 Chengdu, Sichuan, China
[2]Department of Orthopedics, West China Airport Hospital, Sichuan University/the First People's Hospital in Shuangliu District, 610041 Chengdu, Sichuan, China
*Correspondence: zhonggang_zhong@163.com (Gang Zhong)
Published: 20 October 2024

Background: It has been reported that Sirtuin 2 (*SIRT2*) prevents phosphoenolpyruvate carboxykinase 1 (*PCK1*) degradation, which can be involved in aging-induced osteoarthritis (OA), but the molecular mechanism of *SIRT2*/*PCK1* in chondrocytes has not been clarified. Therefore, this study aims to explore the mechanism of *SIRT2*/*PCK1* in chondrocyte inflammation.
Method: To establish the OA model *in vitro*, chondrocytes cultured with interleukin-1β (IL-1β, 10 ng/mL) and manipulation of *SIRT2* and *PCK1* expression in the constructed cells to elucidate the interaction between the two genes. 1,9-Dimethyl-Methylene Blue (DMMB) was used to detect cellular glycosaminoglycan (GAG) content. Inflammatory factor levels were assessed using Enzyme-linked Immunosorbent Assay (ELISA). Apoptosis was detected by osmotic dye. The expression of B-cell lymphoma-2 (Bcl-2), Bcl-2 Associated X (Bax), Wnt Family Member 1 (Wnt1), catenin Beta 1 (β-catenin), Aggrecan, Collagen II, matrix metallopeptidase 13 (MMP-13) proteins in cells were analyzed using Western blot.
Results: *PCK1* gained lower expressions in OA cell models. Overexpression of *PCK1* or S*IRT2* in the IL-1β chondrocyte model of inflammation promoted GAG content, inhibited apoptosis and Wnt/β-catenin protein expression, and lowered the levels of inflammatory factors. *PCK1* silencing was proved to have the opposite effect. *SIRT2* overexpression rescued the increased inflammation, MMP-13 expression, and apoptosis and the decreased Aggrecan and Collagen II expression caused by *PCK1* silencing. *PCK1* silencing also reversed the positive effects of *SIRT2* overexpression on chondrocytes.
Conclusion: *SIRT2* inhibits articular chondrocyte extracellular matrix (ECM) degradation, inflammatory factor expression, and apoptosis via *PCK1*.

Keywords: osteoarthritis; extracellular matrix; Sirtuin 2; phosphoenolpyruvate carboxykinase 1; inflammatory response

Introduction

Osteoarthritis (OA) is a common chronic degenerative disease [1]. Pathological findings show that cartilage damage, inflammatory factors, mechanical injury, and genetic factors are the main predisposing factors [2]. According to the statistics of OA patients in 195 countries worldwide in 2017, more than half of the elderly population suffers from various degrees of OA [3]. An important pathogenic cause of OA is patient cartilage matrix and structure changes [4]. The pathogenesis of OA results in the degradation and metabolic inactivation in the extracellular matrix (ECM) of chondrocytes and the subsequent triggering of cellular senescence and apoptosis [5]. The ECM is mainly composed of Collagen and proteoglycan, and most of its metabolic alterations are regulated by matrix metalloproteinases (MMPs) [6]. Therefore, ECM is also an extremely important consideration in OA prognostic studies. Despite several iterations of current treatments for OA [7], strategies that can target OA to date remain largely ineffective options.

Previous studies indicated that phosphoenolpyruvate carboxykinase 1 (*PCK1*) is involved in important life activities such as apoptosis, inflammatory response, tumor proliferation and invasion, and cancer adipogenesis [8,9]. *PCK1* mediates the onset of inflammatory responses [10, 11]. *PCK1* expression was found to correlate with the development of OA [12], and down-regulation of *PCK1* expression was also demonstrated in a model of OA [13]. Based on these findings, our study focuses on the molecular mechanisms of *PCK1* in OA models and looks for its possibility as a potential therapeutic target. Interestingly, accumulating evidence suggests that Sirtuin 2 (*SIRT2*) mediates the deacetylation of *PCK1* and thus controls glucose metabolism *in vivo* [14]. Also, Chhabra *et al*. [15] demonstrated in obese mice that a reduction in *SIRT2* also pro-

moted *PCK1* loss. *SIRT2* regulates oxidative stress, lipid metabolism, and mitochondrial function in disease [16,17]. It has been shown that *SIRT2* overexpression will attenuate the inflammatory response in patients with diabetic OA [18].

Therefore, in this study, we sought to the evidence that *SIRT2*/*PCK1* regulates the progression of OA inflammation, which offers new insights and targets for treating osteoarthritic diseases.

Materials and Methods

Cell Culture

The human chondrocyte cell line CHON-001 was purchased from the American Type Culture Collection (CRL-2846, ATCC, Rockville, MD, USA) using Dulbecco's Modified Eagle Medium (DMEM, 11965092, Gibco, Waltham, MA, USA) containing 10% fetal bovine serum (FBS, 26140079, Gibco, Waltham, MA, USA) and 1% penicillin/streptomycin (P/S, 15070063, Gibco, Waltham, MA, USA), and incubated at 37 °C and 5% CO_2 for incubation. An *in vitro* cellular model of OA was induced using interleukin-1β (IL-1β) to investigate the chondrocyte inflammatory response further. CHON-001 cell culture medium was replaced with DMEM containing 10 ng/mL IL-1β [19] and incubated for 24 h at 37 °C with 5% CO_2. All cells in this study were confirmed negative for mycoplasma and subjected to short tandem repeat (STR) profile validation.

Plasmid Construction

The overexpression plasmid was created using pcDNA3.1/Puro-CAG-VSFP-CR (40257, Addgene, Teddington, UK) as the plasmid backbone and negative control (NC), and the full-length sequences of *PCK1* and *SIRT2* (**Supplementary File 1**) were cloned into the plasmid backbone. Small interfering RNA (siRNA) encoding oligonucleotides against human *PCK1* (si*PCK1*) was designed with the following targeting sequences:

Forward: 5′-GATCCTTGCCTTGAAGCAAAGAATA-3′

Reverse: 5′-GATTTCGTCGTAACGAAGAACCATA-3′

The scrambled target gene siRNA was used as a negative control (siNC) (A06001, GenePharma, Shanghai, China).

Cell Transfection

CHON-001 cells were transfected with overexpression plasmids using the lipofectamine 3000 transfection kit (L3000150, Invitrogen, Waltham, MA, USA) when CHON-001 cells were cultivated to 70% confluence. Plasmids, liposomes, and Opti-MEM reduced serum medium (31985062, Gibco, Waltham, MA, USA) were mixed proportionally to form DNA-lipid complexes according to manufacturer's instructions. CHON-001 cells were incubated using this complex at 37 °C in 5% CO_2 for 6 h before replacing it with a DMEM complete medium. 2 µg/mL puromycin (P8230, Solarbio, Beijing, China) was screened to identify CHON-001 cells transfected with the target genes, and the expression of the target genes in them was verified using Quantitative Reverse Transcription-polymerase Chain Reaction (RT-qPCR).

For transfection of small interfering RNA sequences, for every 8.4 ng of siRNA, we will use 0.6 µm Hieff-Trans™ *in vitro* transient transfection reagent (40806ES03, Yeasenbiotech, Shanghai, China) and 100 µL of serum-free medium. These reagents will be quickly mixed and incubated at room temperature for 10 min to form siRNA-PEI cationic nucleic acid complexes. Transfection was performed when CHON-001 cells reached 50% confluence. Supplemented with a certain complete medium, the cells were cultured at 37 °C in 5% CO_2 for 72 h, and target gene expression was detected using RT-qPCR.

Grouping

Regarding the grouping of cells, cells cultured in the same batch were randomly divided into 8 groups. Control group: CHON-001 cells normally cultured with DMEM; IL-1β group: CHON-001 cells were cultured with DMEM containing IL-1β (10 ng/mL); IL-1β+NC group: after transfection with the overexpression negative control plasmid, CHON-001 cells were cultured with DMEM containing IL-1β (10 ng/mL); IL-1β+*PCK1* group: after transfection with *PCK1* overexpression plasmid, CHON-001 cells were cultured with DMEM containing IL-1β (10 ng/mL); IL-1β+siNC+NC group: after simultaneous transfection of siRNA and overexpression negative control plasmid, CHON-001 cells were cultured with DMEM containing IL-1β (10 ng/mL); IL-1β+NC+si*PCK1* group: after simultaneous transfection of overexpression negative control and the si*PCK1* plasmid, CHON-001 cells were cultured with DMEM containing IL-1β (10 ng/mL); IL-1β+*SIRT2*+siNC group: after simultaneous transfection of overexpressing *SIRT2* and siRNA negative control plasmid, CHON-001 cells were cultured with DMEM containing IL-1β (10 ng/mL); IL-1β+*SIRT2*+si*PCK1* group: after simultaneous transfection of overexpressing *SIRT2* and si*PCK1* plasmid, CHON-001 cells were cultured with DMEM containing IL-1β (10 ng/mL).

RT-qPCR

The total RNA in the cell was extracted using an RNA extraction kit (R1200, Solarbio, Beijing, China). After removing the genomic DNA, reverse transcription was performed using the cDNA Reverse Transcription Kit (4368813, Thermo Scientific, Waltham, MA, USA). To quantify the amplification products of the target genes in the different tissues and cell lines, reaction systems containing the amplification primers (Table 1, Ref. [13,18]) and

Table 1. Primers of RT-qPCR.

Gene		Sequence (5′ → 3′)
PCK1 [13]	Forward	AAAACGGCCTGAACCTCTCG
	Reverse	ACACAGCTCAGCGTTATTCTC
SIRT2 [18]	Forward	GGTGAACCAGTTGTGTTGTC
	Reverse	CCGTCCTTTCCAGCAGTC
GAPDH [18]	Forward	ACAACTTTGGTATCGTGGAAGG
	Reverse	GCCATCACGCCACAGTTTC

PCK1, phosphoenolpyruvate carboxykinase 1; *SIRT2*, Sirtuin 2; *GAPDH*, Glyceraldehyde-3-Phosphate Dehydrogenase; RT-qPCR, Quantitative Reverse Transcription-polymerase Chain Reaction.

a mixture of SYBRTM Green PCR Master Mix (4344463, Thermo Scientific, Waltham, MA, USA) were assayed using Real-Time PCR Systems (CFX Connect, Bio-Rad, Hercules, CA, USA). Glyceraldehyde-3-Phosphate Dehydrogenase (*GAPDH*) was also selected as an internal reference gene, and the expression levels of all the target genes were normalized and analyzed by $2^{-\Delta\Delta Ct}$ relative quantification [20].

Glycosaminoglycan (GAG) Assay

After lysing the cells using pre-configured lysate (50 mM Tris, pH = 7.9, 10 mM NaCl, 3 mM $MgCl_2$, and 1% Triton X-100 (T8200, Solarbio, Beijing, China)) and proteinase K (P9460, Solarbio, Beijing, China), we prepared 32 mg/L 1,9-Dimethyl-Methylene Blue (DMMB, 341088, Sigma-Aldrich, St. Louis, MO, USA) solution at room temperature, then diluted it two-fold to obtain the DMMB solution using ethanol/GuHCl formate buffer, and stained the samples for 30 min, shielding from light. After color development, the absorbance at 525 nm was measured under a microplate reader (Elx808, BioTek, Winooski, VT, USA). Different dilutions of chondroitin sulfate A were also detected as a standard curve for quantification of GAG in cell lysates. All steps referred to the previous method [21,22].

Enzyme-Linked Immunosorbent Assay (ELISA)

Cell culture supernatants were collected, and cell debris was centrifuged to quantify interleukin 6 (IL-6, 430507, BioLegend, London, UK) and tumor necrosis factor-α (TNF-α, 430207, BioLegend, London, UK) by ELISA kits according to the manufacturer's instructions. Briefly, samples and assay buffer were added proportionally to the plates provided in the kit. The plates were sealed with a plate sealer and incubated with shaking at room temperature for 2 h. Detection antibodies were added and incubated with shaking at room temperature for 1 h, and Avidin-HRP was incubated with shaking at room temperature for 30 min. A substrate solution was added, and the plates were blocked in the dark for 15 min. Absorbance was measured at 450 nm using a microplate reader (Elx808, BioTek, Winooski, VT, USA), and the levels were calculated using a standard curve.

Apoptotic Assay

Cells were fixed using 4% paraformaldehyde (P1110, Solarbio, Beijing, China) and then stained at room temperature for 30 min with the permeability dye Hoechst 33258 (5 µg/mL, H1398, Invitrogen, Carlsbad, CA, USA). Apoptotic cells showed a concentrated blue color in the nucleus as detected by fluorescence microscopy (FSX100, Olympus, Tokyo, Japan) at 100×. We calculated the percentage of apoptotic cells in 10 photographic fields of view for experimental accuracy.

Western Blot

After lysis of cell samples using radioimmunoprecipitation (RIPA, R0010, Solarbio, Beijing, China) and 1% phenylmethanesulfonyl fluoride (PMSF, P0100, Solarbio, Beijing, China), the sample protein solutions were quantified using bicinchoninic acid protein assay (BSA, 23227, Thermo Scientific, Waltham, MA, USA). High-molecular-mass proteins (MW >100 kDa) were separated using 5% Sodium dodecyl sulfate-polyacrylamide gel electrophoresis (SDS-PAGE, P0012A, Beyotime, Shanghai, China), and smaller molecular proteins were separated using 15% SDS-PAGE (P0012A, Beyotime, Shanghai, China). Proteins were then transferred to a 0.45 µm nitrocellulose filter membrane (HATF29325, Millipore, Billerica, MA, USA). After blocking with 5% skim milk for 1 h at room temperature, the primary antibodies (Aggrecan, Mouse, 1 µg/mL, ab3778, 250 kDa, Abcam, Cambridge, UK; Collagen II, Rabbit, 1:1000, ab188570, 141 kDa, Abcam, Cambridge, UK; matrix metallopeptidase 13 (MMP-13), Rabbit, 1:1000, ab51072, 54 kDa, Abcam, Cambridge, UK; B-cell lymphoma-2 (Bcl-2), Rabbit, 1:2000, ab182858, 26 kDa, Abcam, Cambridge, UK; Bcl-2 Associated X (Bax), Rabbit, 1:1000, ab32503, 21 kDa, Abcam, Cambridge, UK; Wnt Family Member 1 (Wnt1), Rabbit, 4 µg/mL, ab63934, 41 kDa, Abcam, Cambridge, UK; β-catenin, Rabbit, 1:10,000, ab32572, 92 kDa, Abcam, Cambridge, UK; GAPDH, Mouse, 1:10,000, ab8245, 36 kDa, Abcam, Cambridge, UK) were incubated for 3 h at room temperature and the secondary antibodies (Goat Anti-Rabbit IgG H&L, 1:10,000, ab205718, Cambridge, UK; Goat Anti-Mouse IgG H&L, 1:10,000, ab205719, abcam, Cambridge, UK) were added to incubated for 1 h at room temperature. To reduce the background noise, the membrane was washed using Tris-Buffered Saline Tween-20 (TBST, T917680, Macklin, Shanghai, China). Enhanced chemiluminescence (ECL) chemiluminescence imager (ChemiDoc, Bio-Rad, Hercules, CA, USA) was used for detection. After the immunoreactive protein bands were detected, the grey values of all bands were analyzed using ImageJ (ImageJ 1.8.0, National Institutes of Health, Bethesda, MD, USA), and the grey values of GAPDH were used as an internal reference to normalize all protein bands.

Statistical Analyses

Comparisons between multiple groups were made using One-way ANOVA, and post-hoc tests were performed using Bonferroni. The Shapiro-Wilk test was used for normality, and the Levene test was used to test the homogeneity of variance. All statistical analyses were realized using GraphPad Prism (GraphPad Prism 8.4.2, La Jolla, CA, USA) and considered statistically significant at $p < 0.05$.

Result

PCK1 Overexpression Inhibited Inflammation and Apoptosis in Inflammatory Chondrocytes and Improved ECM Degradation

We used IL-1β incubated with CHON-001 cells to mimic the pathogenesis of human OA chondrocytes. *PCK1* expression was significantly reduced in IL-1β-treated CHON-001 cells (Fig. 1A, $p < 0.001$). Moreover, we found that *PCK1* expression was significantly increased in the IL-1β+PCK1 group, compared with the IL-1β+NC group, indicating the *PCK1* overexpression plasmid was successfully transfected (Fig. 1A, $p < 0.001$). GAG content was significantly decreased after IL-1β treatment (Fig. 1B, $p < 0.01$). *PCK1* overexpression in IL-1β-induced cells would inhibit GAG loss (Fig. 1B, $p < 0.05$). Consistent with expectation, IL-6 and TNF-α inflammatory factor levels significantly increased after IL-1β treatment (Fig. 1C,D, $p < 0.001$). IL-6 and TNF-α levels were decreased in IL-1β+PCK1 group cells compared to IL-1β+NC group cells (Fig. 1C,D, $p < 0.001$). The destruction of chondrocytes is also one of the factors contributing to the formation of OA, so we detected apoptosis by nuclear staining and found that IL-1β exerted a significant pro-apoptotic effect on chondrocytes (Fig. 1E, $p < 0.001$). This apoptotic effect was reversed by *PCK1* overexpression in IL-1β-treated chondrocytes (Fig. 1E, $p < 0.001$). These findings indicate that IL-1β serves as an effective inducer of OA *in vitro*, and that *PCK1* overexpression can enhance GAG content in inflammatory cells, reduce levels of inflammatory factors, and ameliorate chondrocyte apoptosis.

SIRT2 Overexpression Inhibited Inflammation and Rescued ECM Loss Caused by PCK1 Silencing in Inflamed Chondrocytes

SIRT2 expression was increased after transfected with *SIRT2* overexpression plasmid (Fig. 2A, $p < 0.001$), while *PCK1* silencing had no significant effect on *SIRT2* expression (Fig. 2A). Moreover, *PCK1* expression was significantly down-regulated in IL-1β+NC+si*PCK1* group cells compared to IL-1β+siNC+NC cells (Fig. 2B, $p < 0.01$). Interestingly, we found that *PCK1* expression was significantly upregulated in IL-1β+*SIRT2*+siNC group cells compared to IL-1β+siNC+NC cells (Fig. 2B, $p < 0.001$). Further compared to the IL-1β+*SIRT2*+siNC group cells, *PCK1* expression was significantly down-regulated in IL-1β+*SIRT2*+si*PCK1* group cells (Fig. 2B, $p < 0.001$). These data suggest that *SIRT2* may be an upstream-regulated gene of *PCK1*. Furthermore, we assessed the role of *SIRT2* overexpression with *PCK1* silencing in chondrocytes. *PCK1* silencing would decrease the level of GAG (Fig. 2C, $p < 0.01$); opposite results were shown in overexpressing *SIRT2* (Fig. 2C, $p < 0.05$). *PCK1* silencing led to the elevation of the inflammatory factors IL-6 and TNF-α, whereas *SIRT2* overexpression would be the opposite (Fig. 2D,E, $p < 0.001$). *SIRT2* overexpression would reduce the levels of inflammatory factors in IL-1β+*SIRT2*+si*PCK1* group cells compared to IL-1β+NC+si*PCK1* group cells (Fig. 2D,E, $p < 0.001$).

To verify the loss of ECM by *PCK1* and *SIRT2*, the experiment revealed by Western blot, silencing *PCK1* downregulated the level of Collagen II and Aggrecan proteins. It up-regulated the level of MMP-13 protein (Fig. 3B–E, $p < 0.05$). Opposite results were shown in overexpressing *SIRT2* cells (Fig. 3B–E, $p < 0.05$). Overexpression of *SIRT2* reversed ECM loss caused by *PCK1* silencing in IL-1β-treated chondrocytes (Fig. 3B–E, $p < 0.05$). Similarly, in IL-1β-treated chondrocytes, *PCK1* silencing also abrogated the effects of overexpression of *SIRT2* (Fig. 3B–E, $p < 0.01$). These data suggest that *PCK1* silencing promotes inflammatory factor expression and ECM degradation, whereas overexpression of *SIRT2* rescues the results caused by *PCK1* silencing.

SIRT2/PCK1 Regulated Inflammatory Chondrocyte Apoptosis and Expression of the Wnt/β-Catenin Protein

To further explore the effects of *SIRT2* and *PCK1* on chondrocyte apoptosis in an OA cell model, Hoechst 33258 staining and Western blot revealed that by silencing *PCK1*, the apoptosis of inflammatory chondrocytes was significantly elevated (Fig. 3A, $p < 0.001$), levels of the programmed cell death-associated protein Bax were upregulated, levels of the anti-apoptotic protein Bcl-2 were downregulated, and Wnt1 and β-catenin proteins were significantly upregulated (Fig. 3B,F–I, $p < 0.01$). In contrast, overexpression of *SIRT2* resulted in decreased apoptosis in inflammatory chondrocytes (Fig. 3A, $p < 0.05$), upregulation of Bcl-2 protein, and downregulation of Bax, Wnt1, and β-catenin proteins (Fig. 3B,F–I, $p < 0.01$). *SIRT2* overexpression reversed the effect of *PCK1* silencing (Fig. 3A,B,F–I, $p < 0.05$). Therefore, *SIRT2* overexpression mitigates the impact of *PCK1* silencing on both Wnt/β-catenin protein expression and chondrocyte apoptosis.

Discussion

OA is a common form of arthritis in the population, with more than 500 million people diagnosed with OA throughout the year, according to the 2020 World Health

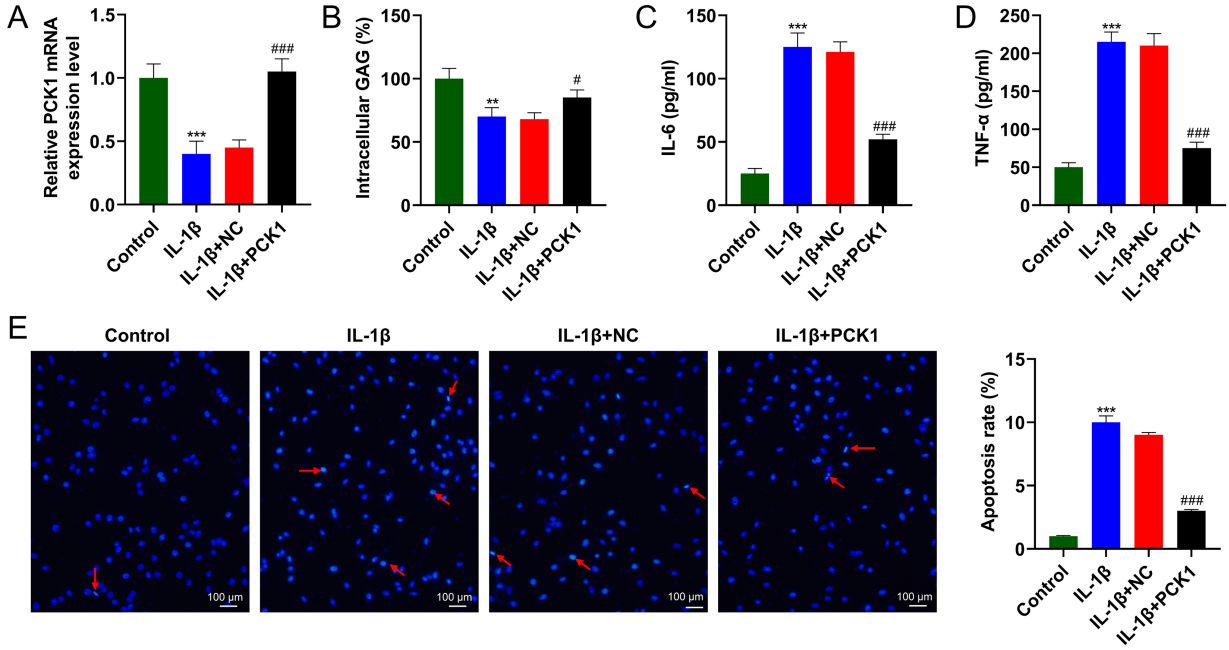

Fig. 1. Effect of *PCK1* overexpression on inflammatory factor levels and apoptosis rate in inflammatory chondrocytes. (A) RT-qPCR detection of *PCK1* expression in a chondrocyte OA model. (B) The detection of GAG content in a chondrocyte OA model by DMMB staining. (C,D) ELISA detection of pro-inflammatory cytokine IL-6 and TNF-α levels in a chondrocyte OA model. (E) The detection of apoptosis in a chondrocyte OA model with Hoechst 33258 stained cell nuclei, arrows indicate an apoptotic cell. $^{**}p < 0.01$, $^{***}p < 0.001$, $^{\#}p < 0.05$; $^{\#\#\#}p < 0.001$; * vs. Control, $^{\#}$ vs. IL-1β+NC, n = 3. Abbreviations: OA, osteoarthritis; DMMB, 1,9-Dimethyl-Methylene Blue; GAG, glycosaminoglycan; ELISA, Enzyme-linked Immunosorbent Assay; IL-6, interleukin 6; TNF-α, tumor necrosis factor-α; IL-1β, interleukin-1β; NC, negative control.

Organization statistical analysis [23]. The current pathological diagnosis of OA is mainly based on the degree of cartilage degeneration [24]. Human cartilage contains a large amount of ECM [25], whose main components are proteoglycan and Collagen [26]. In particular, aiming to enhance the stretching and elasticity of articular cartilage, the Collagen responsible for forming the fibrous network is predominantly type II Collagen [27]. Proteoglycan, an essential source of cartilage resistance, is predominantly Aggrecan, and the basic glycan unit is composed of chondroitin sulfate glycosaminoglycan (CS-GAG) and keratan sulfate chains [28]. In addition, as the level of joint inflammatory factors rises in OA, protease activity increases. The synthesis of Collagen and GAG in the cartilage ECM is degraded and inhibited by matrix metalloproteinases (e.g., MMP-13) [29], which diminishes the function and properties of the ECM [30] and promotes programmed cell death of articular chondrocytes [31]. The influence of these factors on each other will create an unstoppable vicious circle, leading to the rapid deterioration of OA. Thus, early control of OA is now crucial.

PCK1 is an enzyme that plays a key role in the regulation of gluconeogenesis, and its expression supports diabetes, obesity [32], defective mitochondrial function [33], and fatty liver formation [34]. *PCK1* with also has anti-inflammatory activity. It has been shown in hepatitis [35] that *PCK1* expression correlates with the induction of inflammation. There is also evidence that low expression of *PCK1* will also trigger OA by regulating ECM metabolism, leading to cartilage matrix degradation [13]. We found at the cellular level, the assay revealed that the overexpression of *PCK1* in the OA cell model would reverse the action of IL-1β, resulting in a significant increase in the GAG content and a decrease in the levels of the inflammatory factors IL-6 and TNF-α and the rate of apoptosis of the inflamed chondrocytes. The mechanism by which *PCK1* undergoes down-regulation in OA is unclear. Therefore, we explored the upstream genes of *PCK1* in OA action to provide a potential strategy for further application of *PCK1* targets in OA therapy.

Interestingly, we found that overexpression of *SIRT2* increased the *PCK1* expression, while *PCK1* did not affect *SIRT2* expression. Lin *et al.* [14] also indicated that *SIRT2* would target *PCK1* to regulate glycolysis. Moreover, a previous study showed that *PCK1* are substrates of *SIRT2* [36]. Acetylation leads to the reduction of *PCK1* protein stability, protein level, and gluconeogenesis. *SIRT2* is the primary enzyme responsible for *PCK1* acetylation, and inhibition of *SIRT2* activity destroys the stability of *PCK1* [37]. Thus, it was illustrated that *SIRT2* stabilizes *PCK1*. *SIRT2* deacetylates p65 and regulates the expression of specific nuclear factor kappa-B (NF-κB)-dependent genes; silencing *SIRT2*

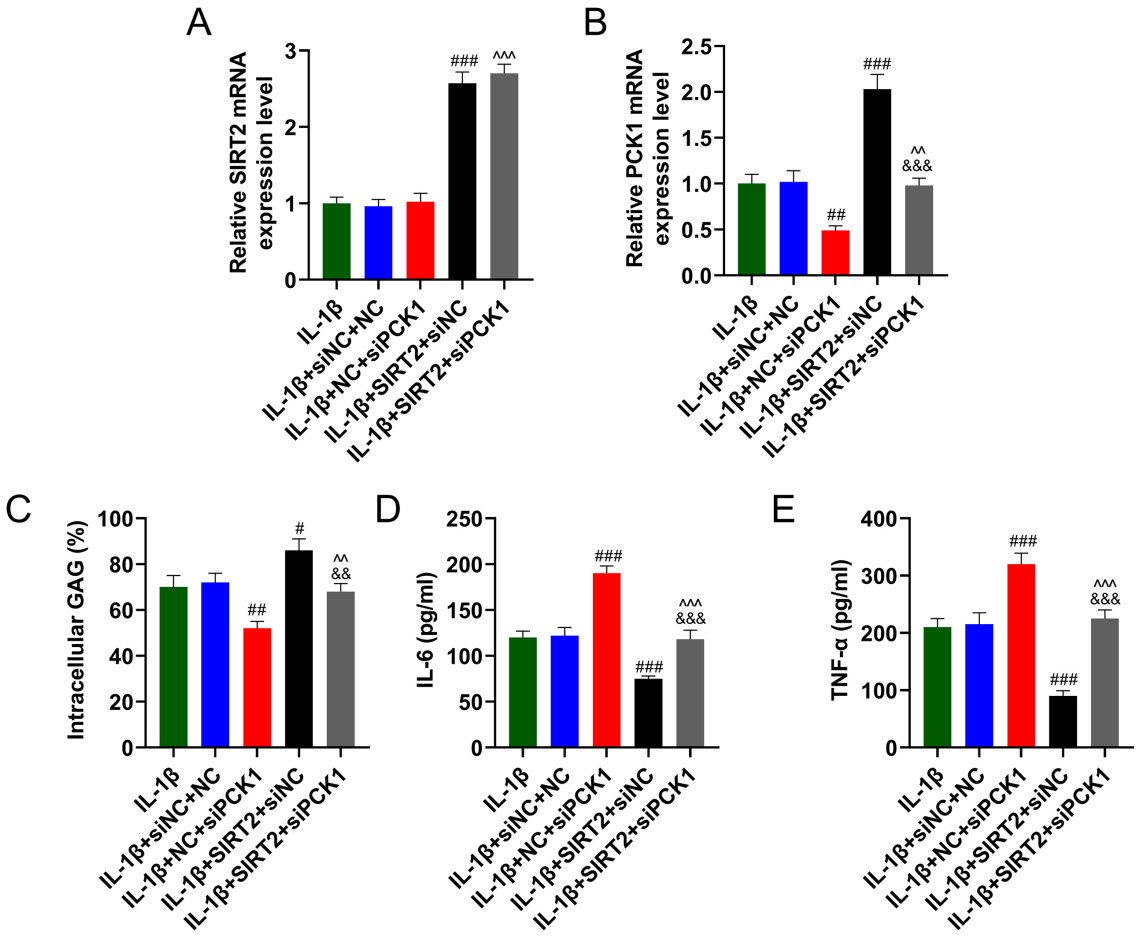

Fig. 2. *SIRT2* overexpression rescued the effect of *PCK1* silencing on GAG and inflammatory factor levels in inflammatory chondrocytes. (A,B) RT-qPCR detection of *SIRT2* and *PCK1* expression in various chondrocyte OA models. (C) The detection of GAG content in each chondrocyte OA model by DMMB staining. (D,E) ELISA detection of pro-inflammatory cytokine IL-6 and TNF-α levels in various chondrocyte OA models. $^{\#}p < 0.05$, $^{\#\#}p < 0.01$, $^{\#\#\#}p < 0.001$, $^{\&\&}p < 0.01$, $^{\&\&\&}p < 0.001$, $^{\wedge\wedge}p < 0.01$, $^{\wedge\wedge\wedge}p < 0.001$; $^{\#}$vs. IL-1β+siNC+NC, $^{\&}$vs. IL-1β+*SIRT2*+siNC, $^{\wedge}$vs. IL-1β+NC+si*PCK1*, n = 3.

reduces lipopolysaccharide-induced microglial activation in BV2 cells and decreases NF-κB activation and nitric oxide synthase levels in macrophages [38]. Silencing *SIRT2* promotes the accumulation of acetylated alpha-tubulin and increases NOD-like receptor thermal protein domain associated protein 3 (NLRP3) inflammasome and mature IL-1β levels, thereby aggravating monosodium urate-induced acute gout arthritis [39]. The presence of *SIRT2* appears to be essential for inflammation. Moreover, a previous study showed that the up-regulation of *SIRT1* expression increased the expression of Bcl-2 and decreased the expression of Bax, MMP-1, and MMP-13, which inhibited the apoptosis and ECM degradation of OA chondrocytes [40]. *SIRT6* overexpression in chondrocytes can reduce the level of MMP-13, and inhibiting MMP activity is expected to block OA progression [41]. Besides, *SIRT2* has also been found to be involved in diabetic OA [18]. Our result showed that *SIRT2* overexpression increased the expression of Bcl-2 and inhibited the Bax and MMP-13 expression caused by IL-1β. Furthermore, our experiments revealed that silencing *PCK1* acted contrary to *SIRT2* overexpression, and *SIRT2* overexpression reversed the effects of *PCK1* silencing on ECM homeostasis, inflammation levels, and apoptosis. Collectively, we can infer that *SIRT2* regulated OA apoptosis and ECM homeostasis by stabilizing *PCK1*. Moreover, a previous study showed that *SIRT2* can be involved in the epigenetic regulation of genes through posttranslational modification of histones, thereby indirectly regulating cell life activities [42]. Therefore, understanding the regulation of *SIRT2* is essential for developing effective OA treatment strategies. Future studies should investigate *SIRT2* expression patterns during OA progression, and identify upstream regulatory factors such as transcription factors and epigenetic modifications.

Previous research has showed that by modulating adenosine 5′-monophosphate (AMP)-activated protein kinase (AMPK)/SIRT1/nuclear factor kappa-B (NF-κB) pathway, cartilage ECM degradation is prevented and in-

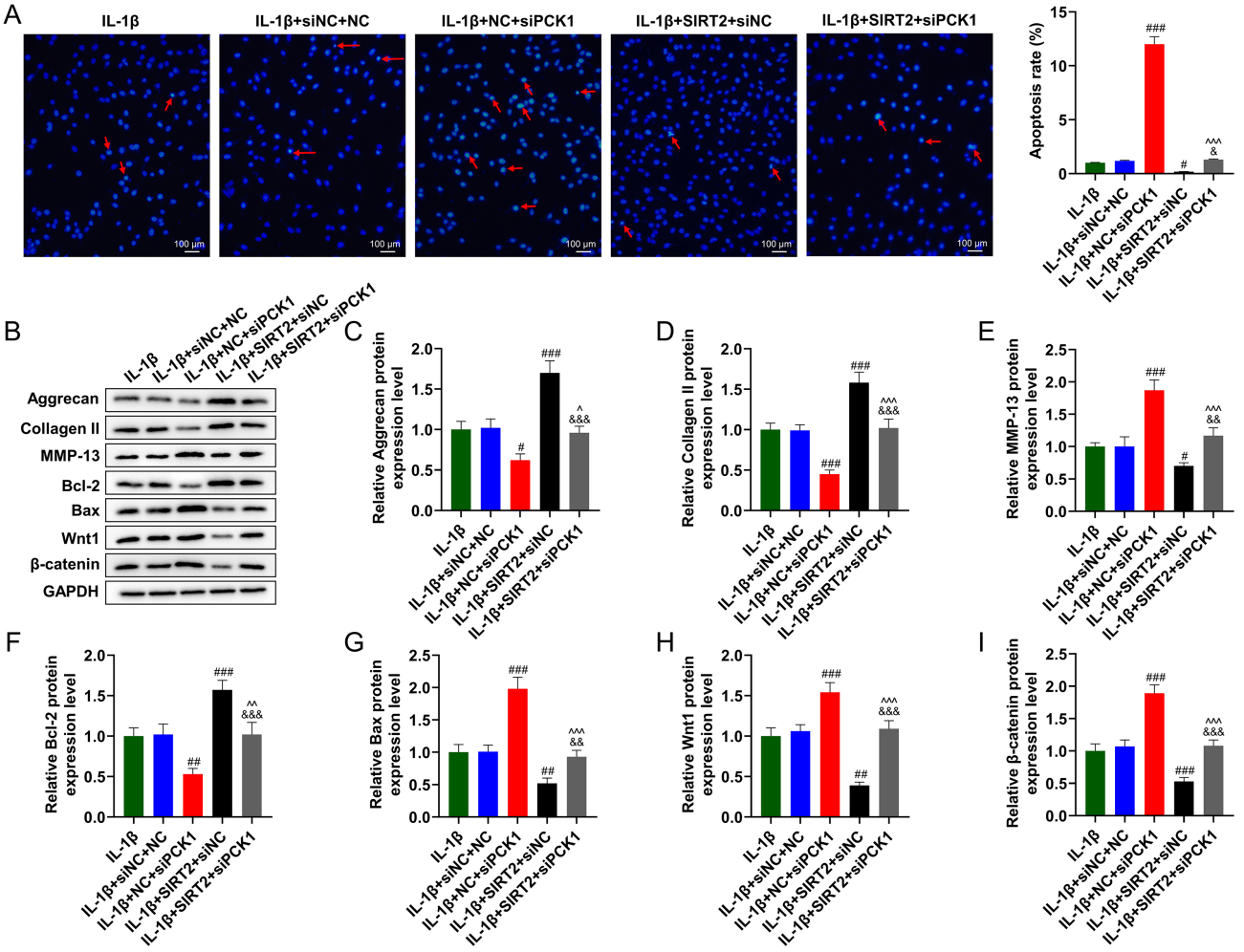

Fig. 3. *SIRT2* overexpression rescued the effects of *PCK1* silencing on apoptosis and ECM degradation in inflammatory chondrocytes. (A) The detection of apoptosis in each chondrocyte OA model with Hoechst 33258-stained cell nuclei; arrows indicate an apoptotic cell. (B–I) Western blot detection of Aggrecan, Collagen II, MMP-13, Bcl-2, Bax, Wnt1, and β-catenin protein in each chondrocyte OA model. $^{\#}p < 0.05$; $^{\#\#}p < 0.01$, $^{\#\#\#}p < 0.001$, $^{\&}p < 0.05$, $^{\&\&}p < 0.01$, $^{\&\&\&}p < 0.001$, $^{\wedge}p < 0.05$, $^{\wedge\wedge}p < 0.01$, $^{\wedge\wedge\wedge}p < 0.001$; $^{\#}$vs. IL-1β+siNC+NC, $^{\&}$vs. IL-1β+*SIRT2*+siNC, $^{\wedge}$vs. IL-1β+NC+si*PCK1*, n = 3. Abbreviations: MMP-13, matrix metallopeptidase 13; Bcl-2, B-cell lymphoma-2; Bax, Bcl-2 Associated X; Wnt1, Wnt Family Member 1; β-catenin, catenin Beta 1.

flammation is inhibited [43]. Therefore, the mechanisms by which *SIRT2*/*PCK1* regulates need to be further explored. *SIRT2* had been shown to function as a mediator of Wnt/β-catenin pathway signaling [44], and overexpressed *PCK1* could also inhibit tumor growth by reducing Wnt/β-catenin signaling [45]. Besides, Wnt/β-catenin signaling controls various molecular functions by regulating the acetylation levels of target proteins [46]. *SIRT1* regulated Wnt signaling by deacetylating histones and β-catenin [47,48]. We found that *SIRT2* overexpression rescued the up-regulation of Wnt/β-catenin protein expression caused by *PCK1* silencing. These results indicated that the Wnt/β-catenin pathway might involved in *SIRT2*/*PCK1* action in OA, which needs more experiments to be identified. However, the relevant molecular mechanisms were not thoroughly examined in this study. Future studies should elucidate the deacetylation site of *SIRT2*-targeted *PCK1*, the effect of this deacetylation on the function of *PCK1*, and the precise mechanism by which *SIRT2*/*PCK1* regulates the activity of the Wnt/β-catenin pathway.

Currently, *SIRT2* is mainly used to screen drugs as therapeutic targets for diseases or as biomarkers to promote diagnosis and prognosis assessment of diseases [42]. Although the experiments have verified the relationship between the two genes in cells, we still need more *in vivo* studies to explore the specific regulatory strategies of *SIRT2* and *PCK1* in the future to solve the related problems more accurately and carefully and promote their clinical application potential targets for disease treatment.

Conclusion

In the present study, we gained insight into the mechanism of *SIRT2*/*PCK1* action in OA. According to our results, *PCK1* may become a downstream-acting substrate of *SIRT2*, which maintains chondrocyte ECM homeostasis and inhibits the activation of inflammatory factors and chondrocyte apoptosis. We therefore speculate that *SIRT2*/*PCK1* may be a new molecular target for OA therapy.

Availability of Data and Materials

The analyzed data sets generated during the study are available from the corresponding author on reasonable request.

Author Contributions

Substantial contributions to conception and design: FZ. Data acquisition, data analysis and interpretation: SQC, CL, LT, GZ. Drafting the article or critically revising it for important intellectual content: all authors. Final approval of the version to be published: all authors. Agreement to be accountable for all aspects of the work in ensuring that questions related to the accuracy or integrity of the work are appropriately investigated and resolved: all authors.

Ethics Approval and Consent to Participate

Not applicable.

Acknowledgment

Not applicable.

Funding

This work was supported by the Orthopedic Special Research Topic of Sichuan Medical Association [2023SAT17].

Conflict of Interest

The authors declare no conflict of interest.

Supplementary Material

Supplementary material associated with this article can be found, in the online version, at https://doi.org/10.24976/Discov.Med.202436189.188.

References

[1] Nelson AE. Osteoarthritis year in review 2017: clinical. Osteoarthritis and Cartilage. 2018; 26: 319–325.

[2] Sharma L. Osteoarthritis of the Knee. The New England Journal of Medicine. 2021; 384: 51–59.

[3] Safiri S, Kolahi AA, Smith E, Hill C, Bettampadi D, Mansournia MA, *et al*. Global, regional and national burden of osteoarthritis 1990-2017: a systematic analysis of the Global Burden of Disease Study 2017. Annals of the Rheumatic Diseases. 2020; 79: 819–828.

[4] Goldring MB, Goldring SR. Osteoarthritis. Journal of Cellular Physiology. 2007; 213: 626–634.

[5] Kumar A, Palit P, Thomas S, Gupta G, Ghosh P, Goswami RP, *et al*. Osteoarthritis: Prognosis and emerging therapeutic approach for disease management. Drug Development Research. 2021; 82: 49–58.

[6] Nagase H, Woessner JF, Jr. Matrix metalloproteinases. The Journal of Biological Chemistry. 1999; 274: 21491–21494.

[7] Arden NK, Perry TA, Bannuru RR, Bruyère O, Cooper C, Haugen IK, *et al*. Non-surgical management of knee osteoarthritis: comparison of ESCEO and OARSI 2019 guidelines. Nature Reviews. Rheumatology. 2021; 17: 59–66.

[8] Sadasivam M, Ramatchandirin B, Balakrishnan S, Selvaraj K, Prahalathan C. The role of phosphoenolpyruvate carboxykinase in neuronal steroidogenesis under acute inflammation. Gene. 2014; 552: 249–254.

[9] Jiang H, Zhu L, Xu D, Lu Z. A newly discovered role of metabolic enzyme PCK1 as a protein kinase to promote cancer lipogenesis. Cancer Communications. 2020; 40: 389–394.

[10] Guo H, Chi Y, Chi N. Bioinformatis analysis reveals possible molecular mechanism of PXR on regulating ulcerative colitis. Scientific Reports. 2021; 11: 5428.

[11] Li H, Li J, Xiao T, Hu Y, Yang Y, Gu X, *et al*. Nintedanib Alleviates Experimental Colitis by Inhibiting CEBPB/PCK1 and CEBPB/EFNA1 Pathways. Frontiers in Pharmacology. 2022; 13: 904420.

[12] Zhong J, Xiang D, Ma X. Prediction and analysis of osteoarthritis hub genes with bioinformatics. Annals of Translational Medicine. 2023; 11: 66.

[13] Gong Z, Wang K, Chen J, Zhu J, Feng Z, Song C, *et al*. CircZSWIM6 mediates dysregulation of ECM and energy homeostasis in ageing chondrocytes through RPS14 post-translational modification. Clinical and Translational Medicine. 2023; 13: e1158.

[14] Lin YY, Lu JY, Zhang J, Walter W, Dang W, Wan J, *et al*. Protein acetylation microarray reveals that NuA4 controls key metabolic target regulating gluconeogenesis. Cell. 2009; 136: 1073–1084.

[15] Chhabra Y, Nelson CN, Plescher M, Barclay JL, Smith AG, Andrikopoulos S, *et al*. Loss of growth hormone-mediated signal transducer and activator of transcription 5 (STAT5) signaling in mice results in insulin sensitivity with obesity. FASEB Journal. 2019; 33: 6412–6430.

[16] Zhang GZ, Deng YJ, Xie QQ, Ren EH, Ma ZJ, He XG, *et al*. Sirtuins and intervertebral disc degeneration: Roles in inflammation, oxidative stress, and mitochondrial function. Clinica Chimica Acta. 2020; 508: 33–42.

[17] Krishnan J, Danzer C, Simka T, Ukropec J, Walter KM, Kumpf S, *et al*. Dietary obesity-associated Hif1α activation in adipocytes restricts fatty acid oxidation and energy expenditure via suppression of the Sirt2-NAD+ system. Genes & Development. 2012; 26: 259–270.

[18] Qu ZA, Ma XJ, Huang SB, Hao XR, Li DM, Feng KY, *et al*. SIRT2 inhibits oxidative stress and inflammatory response in diabetic osteoarthritis. European Review for Medical and Pharmacological Sciences. 2020; 24: 2855–2864.

[19] Wang X, Fan J, Ding X, Sun Y, Cui Z, Liu W. Tanshinone I Inhibits IL-1β-Induced Apoptosis, Inflammation And Extracellular Matrix Degradation In Chondrocytes CHON-001 Cells And Attenuates Murine Osteoarthritis. Drug Design, Development and Therapy. 2019; 13: 3559–3568.

[20] Niesters HG. Quantitation of viral load using real-time amplification techniques. Methods. 2001; 25: 419–429.
[21] Huynh MB, Ouidja MO, Chantepie S, Carpentier G, Maïza A, Zhang G, *et al*. Glycosaminoglycans from Alzheimer's disease hippocampus have altered capacities to bind and regulate growth factors activities and to bind tau. PLoS ONE. 2019; 14: e0209573.
[22] Alluri VK, Kundimi S, Sengupta K, Golakoti T, Kilari EK. An Anti-Inflammatory Composition of *Boswellia serrata* Resin Extracts Alleviates Pain and Protects Cartilage in Monoiodoacetate-Induced Osteoarthritis in Rats. Evidence-based Complementary and Alternative Medicine: ECAM. 2020; 2020: 7381625.
[23] GBD 2021 Osteoarthritis Collaborators. Global, regional, and national burden of osteoarthritis, 1990-2020 and projections to 2050: a systematic analysis for the Global Burden of Disease Study 2021. The Lancet. Rheumatology. 2023; 5: e508–e522.
[24] Yin H, Wang Y, Sun X, Cui G, Sun Z, Chen P, *et al*. Functional tissue-engineered microtissue derived from cartilage extracellular matrix for articular cartilage regeneration. Acta Biomaterialia. 2018; 77: 127–141.
[25] Heinegård D. Fell-Muir Lecture: Proteoglycans and more–from molecules to biology. International Journal of Experimental Pathology. 2009; 90: 575–586.
[26] Luo Y, Sinkeviciute D, He Y, Karsdal M, Henrotin Y, Mobasheri A, *et al*. The minor collagens in articular cartilage. Protein & Cell. 2017; 8: 560–572.
[27] Eyre DR, Weis MA, Wu JJ. Articular cartilage collagen: an irreplaceable framework? European Cells & Materials. 2006; 12: 57–63.
[28] Roughley PJ. The structure and function of cartilage proteoglycans. European Cells & Materials. 2006; 12: 92–101.
[29] Yamamoto K, Okano H, Miyagawa W, Visse R, Shitomi Y, Santamaria S, *et al*. MMP-13 is constitutively produced in human chondrocytes and co-endocytosed with ADAMTS-5 and TIMP-3 by the endocytic receptor LRP1. Matrix Biology. 2016; 56: 57–73.
[30] Hodgkinson T, Kelly DC, Curtin CM, O'Brien FJ. Mechanosignalling in cartilage: an emerging target for the treatment of osteoarthritis. Nature Reviews. Rheumatology. 2022; 18: 67–84.
[31] Lotz MK, Kraus VB. New developments in osteoarthritis. Posttraumatic osteoarthritis: pathogenesis and pharmacological treatment options. Arthritis Research & Therapy. 2010; 12: 211.
[32] Beale EG, Harvey BJ, Forest C. PCK1 and PCK2 as candidate diabetes and obesity genes. Cell Biochemistry and Biophysics. 2007; 48: 89–95.
[33] Hasegawa K, Sakamaki Y, Tamaki M, Wakino S. PCK1 Protects against Mitoribosomal Defects in Diabetic Nephropathy in Mouse Models. Journal of the American Society of Nephrology. 2023; 34: 1343–1365.
[34] Ye Q, Liu Y, Zhang G, Deng H, Wang X, Tuo L, *et al*. Deficiency of gluconeogenic enzyme PCK1 promotes metabolic-associated fatty liver disease through PI3K/AKT/PDGF axis activation in male mice. Nature Communications. 2023; 14: 1402.
[35] Mawed SA, Centoducati G, Farag MR, Alagawany M, Abou-Zeid SM, Elhady WM, *et al*. *Dunaliella salina* Microalga Restores the Metabolic Equilibrium and Ameliorates the Hepatic Inflammatory Response Induced by Zinc Oxide Nanoparticles (ZnO-NPs) in Male Zebrafish. Biology. 2022; 11: 1447.
[36] Zhao S, Xu W, Jiang W, Yu W, Lin Y, Zhang T, *et al*. Regulation of cellular metabolism by protein lysine acetylation. Science. 2010; 327: 1000–1004.
[37] Zhang M, Pan Y, Dorfman RG, Yin Y, Zhou Q, Huang S, *et al*. Sirtinol promotes PEPCK1 degradation and inhibits gluconeogenesis by inhibiting deacetylase SIRT2. Scientific Reports. 2017; 7: 7.
[38] Wang Y, Yang J, Hong T, Chen X, Cui L. SIRT2: Controversy and multiple roles in disease and physiology. Ageing Research Reviews. 2019; 55: 100961.
[39] Zhao Q, Xia N, Xu J, Wang Y, Feng L, Su D, *et al*. Pro-Inflammatory of PRDM1/SIRT2/NLRP3 Axis in Monosodium Urate-Induced Acute Gouty Arthritis. Journal of Innate Immunity. 2023; 15: 614–628.
[40] He DS, Hu XJ, Yan YQ, Liu H. Underlying mechanism of Sirt1 on apoptosis and extracellular matrix degradation of osteoarthritis chondrocytes. Molecular Medicine Reports. 2017; 16: 845–850.
[41] Wu Y, Chen L, Wang Y, Li W, Lin Y, Yu D, *et al*. Overexpression of Sirtuin 6 suppresses cellular senescence and NF-κB mediated inflammatory responses in osteoarthritis development. Scientific Reports. 2015; 5: 17602.
[42] Zhu C, Dong X, Wang X, Zheng Y, Qiu J, Peng Y, *et al*. Multiple Roles of SIRT2 in Regulating Physiological and Pathological Signal Transduction. Genetics Research. 2022; 2022: 9282484.
[43] Wang C, Gao Y, Zhang Z, Chi Q, Liu Y, Yang L, *et al*. Safflower yellow alleviates osteoarthritis and prevents inflammation by inhibiting PGE2 release and regulating NF-κB/SIRT1/AMPK signaling pathways. Phytomedicine. 2020; 78: 153305.
[44] Li C, Zhou Y, Rychahou P, Weiss HL, Lee EY, Perry CL, *et al*. SIRT2 Contributes to the Regulation of Intestinal Cell Proliferation and Differentiation. Cellular and Molecular Gastroenterology and Hepatology. 2020; 10: 43–57.
[45] Xiang J, Zhang Y, Tuo L, Liu R, Gou D, Liang L, *et al*. Transcriptomic changes associated with PCK1 overexpression in hepatocellular carcinoma cells detected by RNA-seq. Genes & Diseases. 2019; 7: 150–159.
[46] You H, Li Q, Kong D, Liu X, Kong F, Zheng K, *et al*. The interaction of canonical Wnt/β-catenin signaling with protein lysine acetylation. Cellular & Molecular Biology Letters. 2022; 27: 7.
[47] Yang Y, Peng W, Su X, Yue B, Shu S, Wang J, *et al*. Epigenomics Analysis of the Suppression Role of *SIRT1* via H3K9 Deacetylation in Preadipocyte Differentiation. International Journal of Molecular Sciences. 2023; 24: 11281.
[48] Zhou Y, Song T, Peng J, Zhou Z, Wei H, Zhou R, *et al*. SIRT1 suppresses adipogenesis by activating Wnt/β-catenin signaling *in vivo* and *in vitro*. Oncotarget. 2016; 7: 77707–77720.